NEM Tubulin Inhibits Microtubule Minus End Assembly by a Reversible Capping Mechanism†

K. K. Phelps and R. A. Walker*

Department of Biology, Virginia Polytechnic Institute and State University, Blacksburg, Virginia 24061-0406

Received September 22, 1999; Revised Manuscript Received February 2, 2000

ABSTRACT: Although microtubule (MT) dynamic instability is thought to depend on the guanine nucleotide (GTP vs GDP) bound to the β-tubulin of the terminal subunit(s), the MT minus end exhibits dynamic instability even though the terminal β-tubulin is always crowned by GTP−α-tubulin. As an approach toward understanding how dynamic instability occurs at the minus end, we investigated the effects of *N*-ethylmaleimide-modified tubulin (NTb) on elongation and rapid shortening of individual MTs. NTb preferentially inhibits minus end assembly when combined with unmodified tubulin (PCTb), but the mechanism of inhibition is unknown. Here, video-enhanced differential interference contrast microscopy was used to observe the effects of NTb on MTs assembled from PCTb onto axoneme fragments. MTs were exposed to mixtures of PCTb (25 μM) and NTb (labeled on ≈1 Cys per monomer) in which the NTb/PCTb ratio varied from 0.025 to 1. The NTb/PCTb mixture had a slight inhibitory effect on the plus end elongation rate, but significantly inhibited or completely arrested minus end elongation. For the majority of mixtures that were assayed (0.1−1 NTb/PCTb ratio), minus end MT length remained constant until the NTb/PCTb mixture was replaced. Replacement with PCTb allowed elongation to proceed, whereas replacement with buffer or NTb caused minus ends to shorten. Taken together, the results indicate that NTb associates with both plus and minus ends and that NTb acts to reversibly cap minus ends only when PCTb is also present. Low-resolution mapping of labeled Cys residues, along with previous experiments with other Cys-reactive compounds, suggests that modification of β-tubulin Cys^{239} may be associated with the capping action of NTb.

Microtubules (MTs)[1] are cytoskeletal polymers composed of heterodimers of α- and β-tubulin. Tubulin dimers assemble head-to-tail to form the protofilaments that comprise the wall of the hollow MT cylinder. Due to this head-to-tail assembly of asymmetrical tubulin subunits, MTs have an intrinsic polarity in which one end is "crowned" with α-tubulin and the other with β-tubulin. This polarity has long been recognized in that one end of a MT (the plus end) elongates 2−3 times faster than the other (the minus end), and more recent evidence indicates that the plus end is crowned by β-tubulin and that the minus end is crowned by α-tubulin (*1*, *2*).

MT assembly in vivo and in vitro occurs by the mechanism of dynamic instability, in which each MT end alternates between phases of elongation and rapid shortening (*3*−*5*). Phase transitions are abrupt, stochastic, and infrequent; the transition from elongation to rapid shortening is termed catastrophe, whereas the reverse is termed rescue (*5*). Dynamic instability is crucial for the cellular function of MTs (reviewed in refs *6* and *7*), and although proteins such as microtubule-associated proteins (MAPs) may modify dynamic instability in vivo (*7*), the mechanism responsible for dynamic instability is intrinsic to the MT. Dynamic instability is thought to depend on the presence or absence of a "GTP cap" at the MT end (reviewed in ref *6*). Each tubulin monomer binds GTP; the GTP bound to α-tubulin is neither exchanged nor hydrolyzed, whereas the GTP bound to β-tubulin is both exchangeable (for unassembled tubulin and perhaps the terminal subunit of the MT) and subject to hydrolysis (after tubulin assembly). During the elongation phase, GTP−tubulin subunits associate with the elongating end and a GTP−tubulin cap at the MT end stabilizes the MT. Loss of this GTP cap, through a mechanism that is not yet clear, exposes GDP−tubulin subunits at the MT end which results in a catastrophe and the MT begins rapid shortening. Recapping of a shortening end by binding of GTP−tubulin subunits to the terminal GDP−tubulin subunits of the MT is thought to generate a rescue, and the MT returns to the elongation phase.

Although dynamic instability may be more crucial for MT plus end functions in vivo (*7*), both MT ends exhibit this behavior in vitro (*4*, *5*). A current paradox is how dynamic instability occurs at the minus end, since the β-tubulin of each terminal subunit is always capped by GTP−α-tubulin. Since understanding differences in dynamics at the two ends will contribute to understanding the fundamental mechanism

† This work was supported by NIH Grant GM52340 (to R.A.W.), a grant-in-aid of research from Sigma-Xi (K.K.P.), and a Graduate Research Development Project (GRDP) grant (K.K.P.) from the Graduate Student Assembly at Virginia Polytechnic Institute and State University.

* To whom correspondence should be addressed: Department of Biology, Virginia Polytechnic Institute and State University, Blacksburg, VA 24061-0406. Phone: (540) 231-3803. Fax: (540) 231-9307. E-mail: rawalker@vt.edu.

[1] Abbreviations: MTs, microtubules; NEM, *N*-ethylmaleimide; NTb, NEM-modified tubulin; PCTb, phosphocellulose-purified tubulin.

10.1021/bi992200x CCC: $19.00
Published on Web 03/18/2000

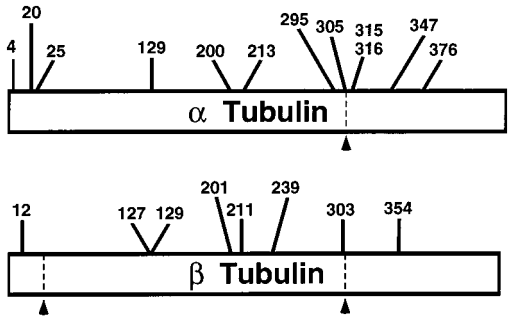

FIGURE 1: Schematic of α- and β-tubulin sequences. The positions of the 20 Cys residues in porcine tubulin are shown. There are 12 Cys residues in the 451-amino acid sequence of α-tubulin and eight Cys residues in the 445-amino acid sequence of β-tubulin (*39*, *40*). Also depicted are the locations of formic acid cleavage sites for each protein (dashed lines indicated by arrowheads).

of dynamic instability, conditions or reagents that affect dynamics at the two ends differently may serve as useful probes for elucidating the mechanism of dynamic instability. One such reagent is *N*-ethylmaleimide (NEM). NEM reacts almost exclusively with Cys residues, and modification of 1−2 Cys per tubulin monomer [for porcine brain tubulin, there are 12 α-tubulin and 8 β-tubulin Cys residues (see Figure 1)] is sufficient to inhibit MT self-assembly (*8*−*10*). However, if NEM-modified tubulin (NTb) is combined with phosphocellulose-purified, unmodified tubulin (PCTb) at certain ratios (typically 0.33−1 NTb/PCTb), plus end assembly continues at near normal rates while minus end assembly is significantly inhibited (*11*, *12*). NTb is routinely used in MT motor research to create MT complexes in which the two ends of the complex can be clearly distinguished and the polarity of motor movement subsequently determined (*13*). Despite a significant amount of work on tubulin Cys residue modification (*14*), the mechanism by which NEM inhibits MT minus end assembly remains unknown. Experiments with other Cys-reactive compounds [e.g., iodoacetamide and *N*,*N*′-ethylenebis(iodoacetamide) (EBI)] also showed that modification of 1−2 Cys residues per monomer inhibits MT self-assembly (*8*, *15*−*17*), but it is not known if this modification also preferentially inhibits minus end assembly. Further, work with some of these compounds indicates that modification of β-Cys^{239} is associated with inhibition of self-assembly (see ref *14* for a review). There is some evidence that NEM reacts with β-Cys^{239} (*18*), but at least one other maleimide derivative reacts with β-Cys^{354} (*19*).

Previous work with NTb either (a) correlated inhibition of MT self-assembly with the number of NEM-reactive Cys residues (*8*−*10*) or (b) entailed viewing individual MT plus and minus ends without knowledge of the extent of modification (*11*, *12*). Further, much of the research with NEM (and other Cys-reactive compounds) either predates the discovery of dynamic instability or did not include an assay for NTb effects on dynamic instability. To address the effect of NTb on dynamic instability, we begin here by determining the effects of a defined NTb preparation (≈1 Cys labeled on each α-tubulin and each β-tubulin monomer) on MT elongation and rapid shortening. MTs were assembled from PCTb (25 μM) onto axoneme fragments in a perfusion chamber, which allowed solution replacement while individual plus and minus end MTs were observed in real time. The initial PCTb solution was replaced by mixtures of PCTb (25 μM) and NTb (0.625−25 μM) in which the fraction of NTb/PCTb varied from 0.025 to 1, and the effect on MT elongation was observed and measured. To examine the effect of NTb on rapid shortening, MTs exposed to NTb/PCTb mixtures were diluted with buffer to induce catastrophe. In addition, low-resolution peptide mapping was performed to distinguish between β-Cys^{239} and β-Cys^{354} as potential sites of NEM modification.

MATERIALS AND METHODS

Tubulin and Axoneme Preparation. PCTb was prepared as described previously (*5*). The pellet produced from sodium glutamate-induced assembly was resuspended in PM buffer [100 mM Pipes, 2 mM EGTA, 1 mM $MgSO_4$, and 1 mM GTP (pH 6.9)], then quick-frozen in liquid nitrogen, and stored at −70 °C. PCTb used for NEM modification was depleted of DTT by passage over a PD-10 column (Pharmacia) equilibrated with PM buffer and 1 mM GTP. These samples were also quick-frozen and stored at −70 °C. DTT-depleted tubulin elongated at the same rate as PCTb [5.83 ± 0.26 μm/min (n = 16) vs 5.53 ± 0.10 μm/min (n = 10) at 25 μM, P > 0.05].

Flagellar axoneme fragments were prepared from *Lytechinus pictus* and used as described previously (*5*).

NEM Modification and Quantitation of Reactive Cys Residues. NEM stock solutions (5×) were prepared fresh in PM buffer. DTT-free tubulin (25 μM final concentration) was modified for up to 30 min on ice with 0.025, 0.05, 0.1, 1, or 5 mM NEM, yielding molar ratios of 1/1, 2/1, 4/1, 40/1, and 200/1, respectively. Control samples were prepared by addition of PM buffer alone. All reactions were quenched by addition of 50 mM DTT, and the mixtures remained on ice for 10−15 min until they were used. Control samples (DTT-depleted PCTb placed on ice for 30 min and the reaction quenched with DTT) elongated at the same rate [5.72 ± 0.34 μm/min (n = 10)] as DTT-depleted PCTb or PCTb (see above).

For quantitation of NEM-reactive Cys residues, tubulin was treated with 0.025, 0.05, 0.1, 0.5, 1, and 5 mM [^{3}H]-NEM (either 2.6 × 10^{13} or 3.4 × 10^{13} cpm/mol) on ice. For each NEM concentration, samples were taken at 5, 10, 15, and 30 min and the modification reactions were quenched by addition of DTT (100 mM final concentration). Reaction mixtures were separated by SDS−PAGE using 95% pure SDS (Sigma catalog no. L-5750) to facilitate resolution of α- and β-tubulin. After being stained with Coomassie Brilliant Blue, tubulin bands were excised from the gel and solubilized with 1 mL of 30% H_2O_2 for 24 h at 60 °C. Each dissolved gel slice was then mixed with 9 mL of scintillation fluid and counted.

Observation of MT Dynamics. MT assembly was observed in perfusion chambers constructed from an acid-washed 22 mm^2 #0 glass coverslip, two pieces of double-sided tape, and a glass slide. The tape was placed on the slide to create a channel; the coverslip was placed on top and pressed onto the tape to give a chamber volume of approximately 6 μL. Sea urchin axoneme fragments were used as seeds to nucleate MT assembly (*5*). Washed axonemes were introduced into the chamber, and after 3 min, the chamber was washed with PM buffer to remove axonemes that had not adhered to the chamber surfaces. Tubulin solutions were prepared immediately prior to use and were diluted to the desired final

concentrations with PM buffer. All tubulin solutions contained 1 mM GTP. MT assembly was initiated by perfusion of PCTb into the chamber, and MTs were identified as plus or minus ended on the basis of the rate of elongation at the two ends of an axoneme. The same chamber was used several (four to five) times with no change in the rate of elongation (data not shown).

Microscopy was performed in a room held at 23−24 °C. Samples were observed by differential interference contrast (DIC) microscopy, using a Nikon SA microscope equipped with a Plan 60×/1.4 NA objective lens, DIC prisms, a 1.4 NA condenser and, a 100 W Hg lamp/fiber optic illumination system. A DAGE VE-1000 newvicon camera provided video imaging and analogue contrast enhancement, and an Argus 10 processor (Hamamatsu) provided digital contrast enhancement, real-time background subtraction, and frame averaging. Images were recorded on S-VHS videotape, and MT elongation and rapid shortening rates were determined from videotape recordings as previously described (*5*).

Mapping of Reactive Cys Residues. Tubulin (40 μg) was treated with 1 mM biotin−NEM for 10 min on ice to label an average of 1 Cys on both α- and β-tubulin. Samples were separated by SDS−PAGE and stained with ChromoPhor dye (Promega), and α- and β-tubulin bands were excised separately from the gel. Protein was eluted from gel slices according to the ChromoPhor protocol, concentrated with a Centricon-30 device, and precipitated with a mixture of chloroform and methanol (*20*). The dried pellets were suspended in 20 μL of 88% formic acid (Fisher) and incubated for 24 h at 37 °C. Samples were then diluted with 480 μL of mQ water, concentrated (Microcon-3 or -10 device), and neutralized by the addition of 2 volumes of 1 M Tris. Samples were separated by tricine-PAGE, and either stained with Coomassie Brilliant Blue or transferred to nitrocellulose membrane and probed with an anti-biotin antibody (Clone BN-34, Sigma) followed by an HRP-conjugated secondary antibody (Pierce). Immunoblots were developed using ECL (Pierce).

RESULTS

Quantitation of NEM Modification of Tubulin. To produce NTb with a defined level of modification, we first quantified the time course of NEM labeling of α- and β-tubulin for a range of NEM concentrations. DTT-depleted tubulin (25 μM) was treated with a 1−200-fold excess of [^{3}H]NEM, and the molar ratio of NEM per monomer (α or β) was determined at 5, 10, 15, and 30 min for each concentration (Figure 2). Labeling occurred almost equally for α- and β-tubulin, increased with increasing NEM concentrations, and appeared to be approaching maximal levels at the higher NEM concentrations (1 and 5 mM) after 30 min. Treatment with 0.025−0.1 mM NEM for 30 min labeled only an average of 0.1−0.5 Cys/monomer. In comparison, treatment with 1 mM NEM for only 10 min labeled an average of almost 1 Cys/monomer, and reached an average labeling of 1.5 Cys/monomer after 30 min. Treatment with the highest NEM concentration, 5 mM, gave an average labeling of 2 Cys/α-tubulin and 1.7 Cys/β-tubulin after 30 min. Treatment with any of the NEM concentrations for 30 min produced NTb that was unable to assemble onto either end of axoneme fragments, and inhibited (0.025, 0.05, and 0.1 mM NEM) or prevented (0.5 and 1 mM NEM) minus end assembly onto axoneme fragments when combined with 25 μM PCTb to produce a 0.5 NT/PCTb mixture (data not shown).

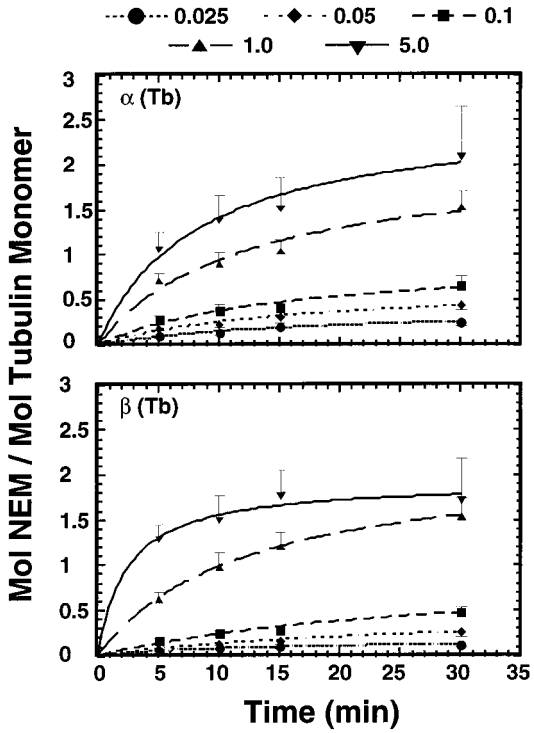

FIGURE 2: Quantitation of NEM-reactive Cys residues in α- and β-tubulin. Tubulin (25 μM DTT-depleted tubulin) was treated with 0.025, 0.05, 0.1, 1.0, and 5.0 mM [^{3}H]NEM on ice for the indicated times. Samples were subjected to SDS−PAGE; α- and β-tubulin bands were excised from the gel and solubilized with H_2O_2, and the amount of radioactivity was counted. Each data point represents the mean of six experiments. SEM bars point up for 0.1, 1, and 5 mM and down for all others. Increase over the time course is indicated (dotted line, 0.025; short-dashed line, 0.05; medium-dashed line, 0.1; long-dashed line, 1.0; and solid line, 5.0).

Effect of NTb on Assembled MT Ends. To determine how NTb affected the dynamics of existing MTs, we used video-enhanced differential interference contrast light microscopy to observe individual MTs. For these experiments, 25 μM PCTb was first added to a chamber containing axoneme fragments to assemble MTs onto both axoneme ends. After 2−3 min, the PCTb was replaced with mixtures of PCTb and NTb in which the PCTb concentration was held constant at 25 μM and the NTb concentration was varied from 625 nM to 25 μM. The NTb used in these experiments was prepared so that an average of ≈1 Cys per monomer was modified (1 mM NEM for 10 min; see Figure 2). These treatment conditions are essentially the same used in previous work with NTb (*12*), although the corresponding level of modification in that work was not reported. No MTs of either polarity were observed when this 25 μM NTb preparation was incubated with axonemes in the absence of PCTb (data not shown). Example plus and minus end MT life history plots are shown in Figure 3 for MTs that were switched from PCTb to a 0.25 NTb/PCTb mixture. For both ends, the life histories that are depicted are representative of all MTs switched from PCTb to NTb/PCTb; i.e., plus end MTs continued to elongate at or near PCTb elongation rates, while minus end MTs ceased elongation and remained constant in length. MT elongation rates following introduction of the NTb/PCTb mixture were measured, and the results are shown

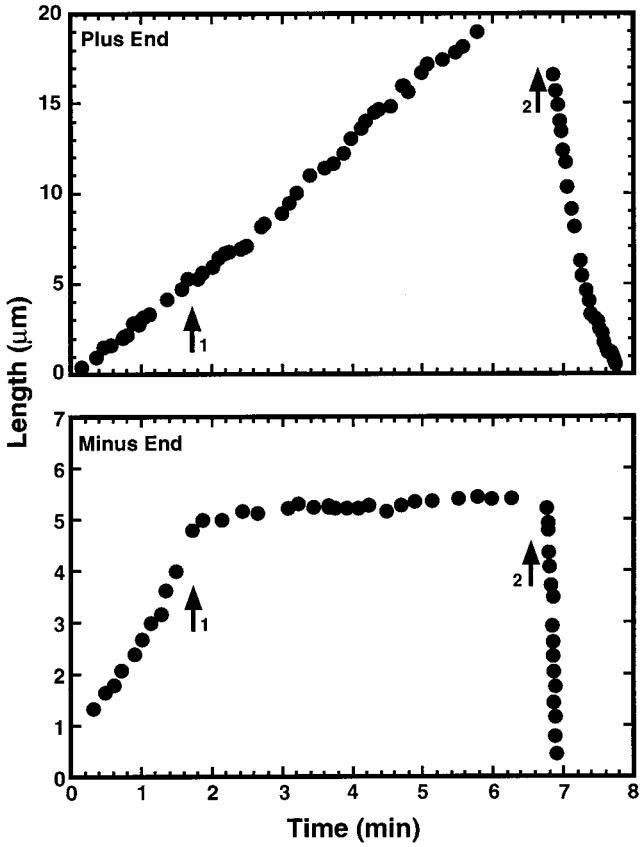

FIGURE 3: Life history plots of MTs switched from PCTb to a 0.25 NTb/PCTb mixture. Representative life history (length vs time) plots of a plus end MT (top) and a minus end MT (bottom) in which elongating MTs were exposed to NTb. MTs were initially assembled onto axoneme fragments from PCTb (25 μM), and this solution was replaced at the indicated time (arrow 1) with 2−3 chamber volumes of a 0.25 NTb/PCTb mixture (25 μM PCTb). After approximately 5 min (arrow 2), the NTb/PCTb mixture was replaced with PM buffer to induce rapid shortening. The plus end MT in this example grew out of the field of view just prior to dilution.

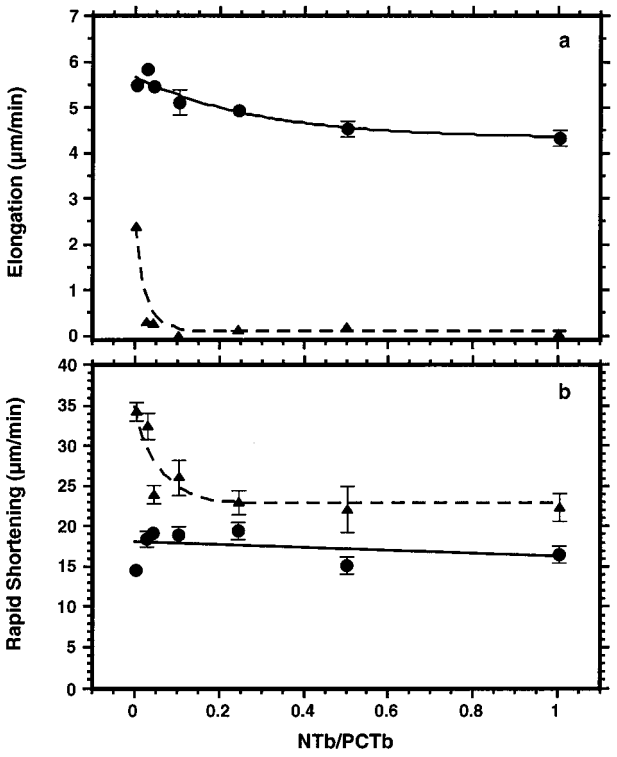

FIGURE 4: MT elongation and dilution-induced rapid shortening rates as a function of the NTb/PCTb ratio. Solution replacement experiments were performed as described in the legend of Figure 3 and Materials and Methods. PCTb (25 μM) was mixed with NTb to generate the indicated NTb/PCTb ratios and added to elongating MTs. Elongation (a) and subsequent dilution-induced shortening (b) rates are plotted for plus (●) and minus ends (▲) for each NTb/PCTb mixture. Each point represents the mean of 8−20 MTs. Error bars (standard error of the mean) were within symbol size except as indicated.

in Figure 4a. At the plus end, 0.025−0.1 NTb/PCTb mixtures had no significant effect on elongation rate (compared to 25 μM PCTb), whereas 0.25−1 NTb/PCTb mixtures significantly reduced the elongation rate by ≈20% ($P < 0.05$ for a 0.25 NTb/PCTb mixture, $P < 0.01$ for 0.5 and 1 NTb/PCTb mixtures). At the minus end, all NTb/PCTb mixtures significantly ($P < 0.001$) inhibited elongation. It is possible that some minus end elongation occurred with the 0.025 and 0.04 NTb/PCTb mixtures, both of which gave elongation rates of about 0.3 μm/min, but this rate is very close to the limit that can be measured accurately in the in vitro MT assembly assay (*5*). Regardless of whether elongation was completely arrested, minus end MTs in the presence of any NTb/PCTb mixture examined never underwent a catastrophe. Even when individual minus ends were observed for 30 min, no significant change in MT length could be detected [for a 0.25 NTb/PCTb mixture, the elongation rate was 0.02 ± 0.01 μm/min ($n = 9$)]. If 25 μM NTb, which did not assemble directly onto axonemes, was perfused into the chamber instead of a NTb/PCTb mixture, however, both plus and minus ends converted to rapid shortening within seconds of the perfusion and shortened all the way back to the axoneme. Plus and minus end MTs exposed to 25 μM NTb shortened at rates of 19.0 ± 2.4 ($n = 13$) and 24.9 ± 1.5 μm/min ($n = 5$), respectively. The plus end shortening rate was not significantly different ($P > 0.05$) from the dilution-induced shortening rates of PCTb MTs (see Figure 4b). However, the minus end shortening rate in the presence of NTb was reduced by 30% ($P < 0.01$) compared to the dilution-induced shortening rates of PCTb MTs.

No catastrophes and hence no rescues were observed during the course of these experiments, presumably because the PCTb concentration was sufficiently high that the frequency of catastrophe was essentially zero. Therefore, to determine if NTb affected rapid shortening rates, MT elongation in the presence of NTb/PCTb mixtures was typically observed for ≈5 min, and the solution was then replaced with PM buffer to induce MT shortening (Figure 4b). All MTs converted to rapid shortening within ≤5 s of the perfusion, and shortening rates of plus end MTs exposed to the various NTb/PCTb mixtures were not significantly different ($P > 0.05$) from those of MTs that had been assembled in the presence of only PCTb. However, minus end MTs exposed to 0.04−1 NTb/PCTb mixtures shortened significantly more slowly (by 25−35%, $P < 0.01$) than MTs assembled from only PCTb. Given the inhibitory effect of NTb on both plus end and minus end elongation, we next characterized the effect of NTb on the rates of association (k_2^e) and dissociation (k_{-1}^e) of elongation. The rate of elongation (v^e) is equal to (k_2^e)([tubulin]) − k_{-1}^e, and k_2^e and k_{-1}^e can be determined by linear regression analysis of elongation rate versus tubulin concentration data (*5*). How-

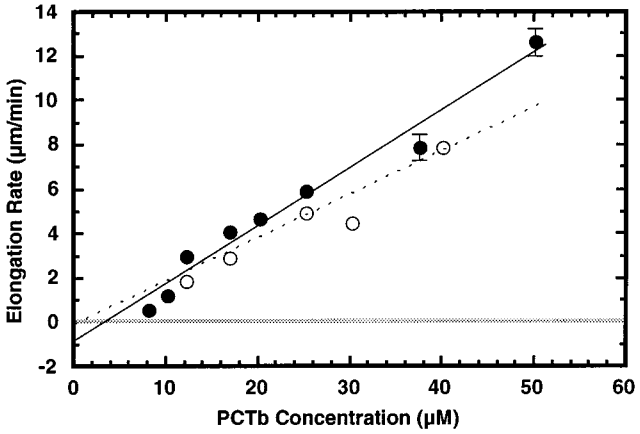

FIGURE 5: Plus end rate of elongation as a function of tubulin concentration. Mean elongation rates of plus end MTs assembled from PCTb (●) and a 0.25 NTb/PCTb mixture (○) are plotted as a function of PCTb concentration. The slopes for each were determined by linear regression analysis of the entire data set ($n^{PCTb} = 81$, $n^{NTb/PCTb} = 59$). Error bars for the means correspond to the standard error of the mean and were typically within the symbol size. Linear regression analysis yielded a slope of 0.262 ± 0.012 μm μM^{-1} min^{-1} for PCTb and 0.189 ± 0.013 μm μM^{-1} min^{-1} for the 0.25 NTb/PCTb mixture. The *Y*-intercept values for PCTb and the 0.25 NTb/PCTb mixture were -0.78 ± 0.33 and 0.24 ± 0.35 μm/min, respectively. Since the 0.25 NTb/PCTb mixture *Y*-intercept was slightly positive, the linear regression was recalculated to constrain the fit through the origin (the lowest possible value for k_{-1}^e). This adjusted the slope to 0.197 ± 0.004 μm μM^{-1} min^{-1}.

ever, since minus end elongation rates were at or near the limits that could be accurately measured, we were unable to determine minus end rate constants in the presence of NTb. Rate constants were therefore determined for plus end MTs assembled from PCTb and from a 0.25 NTb/PCTb mixture (Figure 5). This ratio was selected since it was the lowest proportion of NTb that caused a statistically significant decrease in elongation rate compared to that of PCTb (Figure 4a). Data for the 0.25 NTb/PCTb mixture were plotted using the concentration of PCTb in the mixture. The lowest PCTb concentration that supported plus end elongation was 8 μM, while the lowest PCTb concentration that could support plus end elongation in the presence of NTb was 12 μM. On the basis of linear regression analysis of the data shown in Figure 5, the plus end k_2^e value for PCTb was 7.1 ± 0.3 μM^{-1} s^{-1}, while the k_2^e value for the 0.25 NTb/PCTb mixture was 5.4 ± 0.1 μM^{-1} s^{-1}. For PCTb, the calculated k_{-1}^e value for the plus end was -21.2 ± 9.0 s^{-1}, while the k_{-1}^e for the 0.25 NTb/PCTb mixture was 0 s^{-1} (see the legend of Figure 5).

Elongation of NTb-Arrested MTs. To determine if NTb-arrested minus ends could be subsequently elongated, experiments were performed as described in the legend of Figure 3 except that NTb/PCTb mixtures were subsequently replaced with PCTb (25 μM). Representative MT life history plots for plus and minus end MTs subjected to this triple-replacement protocol are presented in Figure 6. The data show that minus ends arrested by a 0.025, 0.1, or 0.25 NTb/PCTb mixture resumed elongation at the rate predicted for 25 μM PCTb. However, when this PCTb was subsequently flushed from the chamber to induce MT rapid shortening, a surprising pattern was observed for every ($n = 47$) plus end MT that was analyzed. When dilution-induced shortening took place, plus end MTs consistently exhibited a brief pause in shortening upon reaching the last region of the MT that was assembled in the presence of the NTb/PCTb mixture. This pause was never observed for minus end MTs during the course of these experiments. Although detectable on life history plots, the pauses were so brief that the mean rate for the rapid shortening episode [16.38 ± 0.71 μm/min ($n = 47$)] was not significantly different ($P > 0.05$) from the shortening rates measured for MTs assembled completely from PCTb or from PCTb and a NTb/PCTb mixture (Figure 4b).

Mapping of Critical Cys Residues. Given the evidence pointing to β-Cys^{239} as being critical for assembly (*14*, *21*) and the fact that a maleimide derivative has been found to react with β-Cys^{354} (*19*), we sought to distinguish between these two residues as possible targets of NEM. To obtain a low-resolution map of reactive Cys residues, tubulin was treated with biotin−NEM [which performed in a manner identical to that of NEM in assembly assays (data not shown)], and α- and β-tubulin were separated by SDS−PAGE. The proteins were then digested with formic acid, which cleaves between Asp and Pro residues. As depicted in Figure 1, there is one such site in α-tubulin (^{306}DP^{307}), and cleavage yields two fragments: one 34 kDa fragment (containing eight Cys residues) and one 16 kDa fragment (containing four Cys residues). β-Tubulin has two formic acid cleavage sites (^{31}DP^{32} and ^{304}DP^{305}) that should yield three fragments: one 30 kDa fragment (containing six Cys residues), one 16 kDa fragment (containing one Cys residue), and one 3 kDa fragment (containing one Cys residue). Following digestion, fragments were separated by SDS−PAGE, transferred to nitrocellulose membrane, and probed with an antibody against biotin (Figure 7). In addition to the undigested labeled proteins, the anti-biotin antibody recognized the α-tubulin 34 kDa fragment and the β-tubulin 30 kDa fragment, but did not detect the 16 kDa fragments of either protein (the β-tubulin 3 kDa fragment was lost during SDS−PAGE). Taken together, these results indicate that α-Cys^{315}, α-Cys^{316}, α-Cys^{347}, α-Cys^{376}, and β-Cys^{354} were not labeled by NEM and are therefore not associated with the action of NTb. In addition to the expected products for β-tubulin, ≈50 and ≈27 kDa fragments were generated by formic acid digestion. The ≈50 kDa fragment was recognized by the anti-biotin antibody and probably corresponds to amino acids 31−445, but it is not clear which β-tubulin sequence corresponds to the ≈27 kDa fragment.

DISCUSSION

The most dramatic effect of NTb in these experiments was the near-to-complete arrest of minus end elongation (Figures 3, 4, and 6). Minus end elongation was completely blocked over a 10-fold range of NTb/PCTb ratios (0.1−1 NTb/PCTb), and at relatively high total tubulin concentrations (25 μM PCTb and 25 μM NTb) (Figure 4). The inhibition of minus end elongation indicates that NTb associates with this end of the MT, and provides an explanation for the previously documented absence of minus end MTs on stabilized seeds in NTb/PCTb mixtures (*11*, *12*). However, the proportion of NTb sufficient to arrest minus end elongation in the current experiments (Figure 4a) was 10-fold lower (0.1 vs 1) than that found for complete inhibition of minus end assembly onto stabilized MT seeds in the same earlier

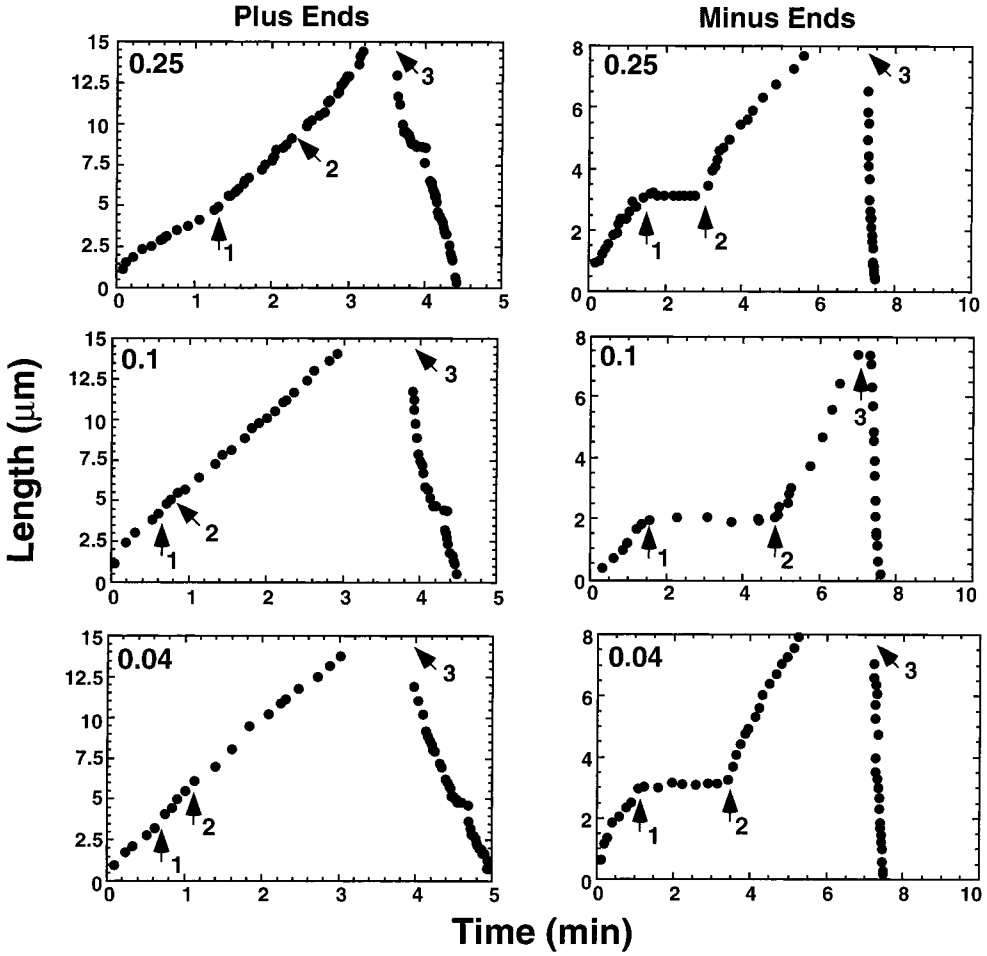

FIGURE 6: Life history plots of MTs switched from PCTb to a NTb/PCTb mixture to PCTb. MTs were assembled from 25 μM PCTb for 1−2 min, and this solution was replaced with a 0.25 NTb/PCTb mixture (25 μM PCTb) at the time indicated by arrow 1. This mixture was then replaced with PCTb (25 μM) at the time indicated by arrow 2, and finally, the chamber volume was replaced with 6 volumes of PM buffer at the time indicated by arrow 3. Example plus and minus end MTs for three different NTb/PCTb mixtures (0.25, 0.1, and 0.04) are shown. Note the brief pause in shortening for plus end MTs upon reaching the length corresponding to arrow 2.

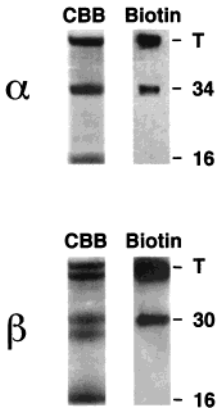

FIGURE 7: Mapping of reactive Cys residues in α- and β-tubulin. Tubulin was modified with biotin−NEM and digested with formic acid as described in Materials and Methods. Digested α- and β-tubulin were separated by SDS−PAGE and either stained with Coomassie Brilliant Blue (CBB lanes) or transferred to nitrocellulose and probed with an antibody against biotin (Biotin lanes). The positions of undigested tubulin (T) and the major formic acid-generated fragments of tubulin are indicated by the molecular mass in kilodaltons. In addition to the expected products for β-tubulin, fragments of ≈50 and ≈27 kDa were also generated by formic acid digestion.

reports. This difference may be due to different NTb modification levels (unknown in the earlier studies vs ≈1 Cys per monomer here) or to differences between stabilized and dynamic MT ends.

NTb not only arrested minus end elongation but also stabilized minus end MTs against catastrophe. For PCTb, there is an inverse relationship between elongation rate and catastrophe frequency, and MTs that fail to elongate or elongate very slowly (≤0.30 μm/min) convert to rapid shortening within seconds (*5*, *22*). However, minus end MTs stabilized by NTb were never observed to convert to rapid shortening even when followed for up to 30 min (the longest period of continuous observation). Thus, NTb appears to form a "cap" at the minus end that simultaneously limits productive addition of PCTb subunits and stabilizes against the "normal" mechanism of catastrophe. Dilution of NTb/PCTb mixtures with either buffer or NTb alone (25 μM) induced rapid shortening (Figures 3, 4, and 6), indicating that NTb-dependent stabilization of minus ends is reversible and that NTb subunits dissociate from the minus end. This result also explains the previous observation that exposing stabilized MT seeds to NTb does not subsequently inhibit MT assembly onto the seeds after the NTb is removed (*11*). The fact that NTb alone cannot support MT elongation or prevent minus ends from converting to rapid shortening suggests that NTb alone is not sufficient to create or maintain the minus end cap. The requirement for NTb and PCTb

subunits in solution suggests that cap maintenance involves PCTb and NTb association and dissociation at the minus end with no net change in MT length.

Analysis of NTb effects on rapid shortening also provides evidence for association of NTb with shortening minus (but not plus) ends. The rate at which minus ends shortened in the presence of 25 μM NTb was slower than the rates of those exposed to buffer alone. Since the rapid shortening rate for MTs assembled from PCTb is identical following spontaneous or dilution-induced conversion to rapid shortening (*5*, *22*), the reduced shortening rate observed with 25 μM NTb suggests that NTb associates with shortening minus ends and thereby slows subunit dissociation during this phase. A surprising observation, consistent with this interpretation, was that minus end MTs exposed to NTb/PCTb mixtures prior to dilution-induced shortening also showed a reduced rate of rapid shortening (Figure 4b). Since no significant polymer formation occurred at these minus ends in the presence of NTb/PCTb, the most likely explanation for the reduced shortening rate at the minus ends is that some residual NTb remained after dilution, and that even low concentrations of NTb may decrease the rate of minus end shortening.

Although the most dramatic effect of NTb was stabilization of the minus end, NTb also inhibited plus end elongation. Previous studies with 0.33−1 NTb/PCTb mixtures found little or no inhibitory effect on plus end elongation rate (*11*, *12*). In comparison, we found that while NTb had no significant effect on plus end elongation rate at ≤0.1 NTb/PCTb ratios, mixtures with ≥0.25 NTb/PCTb ratios caused significant inhibition of plus end elongation (Figure 4). The reason for this slight difference is not clear but may, as mentioned above, be due to NTb modification level differences between the earlier studies and the present work. The decrease in elongation rate in the presence of NTb (see Figure 4) indicates that NTb associates with the plus end, and this conclusion is supported by the inhibitory effect of NTb on plus end association and dissociation rate constants (Figure 5). The association rate constant for PCTb was reduced by 24% when PCTb was supplemented with NTb to give a 0.25 NTb/PCTb mixture, and the dissociation rate was reduced to 0 (actually slightly positive as fit by linear regression). The reduced association rate constant suggests that NTb inhibits the rate at which PCTb adds to the plus end. Although the mechanism of such inhibition is not clear, NTb at the MT end may directly block the subsequent addition of PCTb subunits. The reduction in the dissociation rate constant indicates that tubulin subunits (NTb and/or PCTb) dissociate slowly from the plus end, and suggests either that NTb may dissociate more slowly than PCTb or that NTb at the MT end may prevent PCTb subunits from dissociating. Although there was no evidence for plus end stabilization for the NTb/PCTb mixtures used in the experiments described here, it remains possible that NTb in excess of PCTb may produce stabilization of the plus end.

Continued elongation of plus end MTs exposed to NTb/PCTb mixtures suggests that NTb may be incorporated into these elongating ends, which may affect the shortening rate when these MTs disassembled following dilution. Plus end MTs subjected to dilution-induced rapid shortening were composed of two regions: an axoneme-proximal region assembled from PCTb and a distal region assembled from NTb/PCTb mixtures (Figures 3 and 4b). For each mixture, the overall plus end rapid shortening rate was not significantly different from that of MTs assembled entirely from PCTb, and there was no difference in shortening rate between the two regions. These results suggest either that NTb is not incorporated into an elongating plus end or, if incorporated, that NTb does not significantly alter the interactions between neighboring subunits during disassembly. However, triple-replacement experiments (Figure 6) revealed a more complicated situation. MTs in these experiments consisted of three regions: an axoneme-proximal region assembled from PCTb, a central region assembled from a NTb/PCTb mixture, and a distal region assembled from PCTb. During dilution-induced shortening, every ($n = 47$) plus end MT that was observed exhibited a brief pause at the interface between the distal PCTb region and the central NTb/PCTb region, whereas no pauses were observed for minus end MTs exposed to the same conditions. Pauses during plus end rapid shortening occurred only at the interface and not throughout the entire central region of the MT where NTb could have been incorporated. One possible explanation for the pause is that NTb at the MT end may be buried by the newly added PCTb, although why this would occur only at the interface and not continually during elongation of the NTb/PCTb region is not clear. In any case, the pause suggests that NTb was incorporated into these MTs and provides further evidence that NTb associates with plus ends. In addition, the pause suggests that NTb dissociates more slowly than GDP−tubulin. Efforts to visualize NTb incorporation by immunofluorescent methods using biotin−NEM and anti-biotin antibodies, or to quantify NTb co-assembly by sedimentation of MTs assembled in the presence of [^{3}H]-NEM-modified NTb, have so far been unsuccessful.

How does NEM modification create a tubulin subunit that is able to cause the effects observed at both MT ends? Answering this question depends ultimately on identification of the critical NEM-reactive Cys residues. A complicating factor in understanding how NTb affects MT dynamics is that α- and β-tubulin are labeled almost equivalently by NEM (*9*, *10*) (Figure 2). It is not clear which α-Cys residues react with NEM (or other SH-reactive compounds), but our low-resolution mapping (Figure 7) indicates that α-Cys^{315}, α-Cys^{316}, α-Cys^{347}, and α-Cys^{376} can be eliminated as candidates for NEM modification. In contrast to α-tubulin, several β-tubulin Cys residues are known to react with SH-modifying reagents. These fall into two categories: residues proximal to the E-site (Cys^{12}, Cys^{201}, and Cys^{211}) and residues in the vicinity of the colchicine-binding site (Cys^{239} and Cys^{354}). Analysis of the dimer structure (*23*) indicates that none of these β-Cys residues are readily accessible. However, the structure is based on tubulin within a Zn^{2+}-sheet protofilament, and a free dimer in solution may have a sufficiently different conformation to allow NEM access to these residues. This possibility is demonstrated by the fact that α-Cys^{295} can be cross-linked to N-site GTP (*24*), even though the distance between the two appears too great in the structure (*23*).

In terms of E-site Cys residues, β-Cys^{12} can be cross-linked to either β-Cys^{201} or β-Cys^{211} by EBI (*25*), but only in the absence of free GTP. In addition, an E-site nucleotide can be cross-linked to β-Cys^{12} (*26*, *27*) or β-Cys^{211} (*27*). There are several arguments against these E-site Cys residues as

the NEM target(s) in the study presented here. First, all NEM labeling was carried out with excess free GTP, which suppresses the ability of certain SH-reactive compounds (e.g., EBI) to react with E-site Cys residues (*25*), but does not affect NEM modification of tubulin (*10*). Second, NEM does not affect tubulin's ability to bind or exchange GTP (*9*, *10*). Finally, spin-label studies indicate that the two most reactive SH groups are at least 10 Å from the E-site GTP (*10*). Thus, even though low-resolution mapping (Figure 7) does not eliminate β-Cys^{12}, β-Cys^{201}, or β-Cys^{211}, previous work appears to exclude these as targets of NEM in this study.

In terms of the Cys residues near the colchicine-binding site, there has been extensive work on the relationship between colchicine binding and β-Cys^{239} and β-Cys^{354} (reviewed in ref *14*). There is now substantial evidence that β-Cys^{354} is involved in interactions with the A ring of colchicine (*28*), whereas β-Cys^{239} may be masked by colchicine binding to tubulin and may not necessarily interact directly with colchicine (*18*, *21*, *28*). β-Cys^{239} and β-Cys^{354} can be cross-linked by EBI in the presence of free GTP (*29*), but formation of this cross-linked product, and NEM modification of tubulin, are inhibited by prior binding of colchicine (*18*). These two residues were localized to a region near the intradimer interface between α- and β-tubulin via photoaffinity experiments (*30*, *31*), and this location was recently confirmed with the determination of the tubulin dimer structure (*23*). Low-resolution mapping (Figure 7) suggests that of the two, β-Cys^{239} is the more likely target of NEM. The assignment of β-Cys^{239} as the critical NEM-reactive Cys residue is supported by experiments with at least two additional reagents (2,4-dichlorobenzyl thiocyanate and T138067) that show specificity for this residue (*21*, *32*). Modification of tubulin with either agent inhibits MT self-assembly (minus end-specific inhibition was not examined), and is also inhibited by colchicine (*21*, *32*). Interestingly, the stabilization of MT minus ends by NTb is similar to that reported for the tubulin−colchicine complex in vitro (*33*), although the tubulin−colchicine complex stabilizes plus ends as well as minus ends (*34*, *35*), and preferentially and irreversibly inhibits minus end disassembly following dilution (*36*). Some of these differences could be related to the fact that colchicine spans the intradimer contact and interacts with α- as well as β-tubulin (*30*, *31*, *37*, *38*).

Taken together, the common ability of NEM and other SH-modifying reagents to inhibit tubulin self-assembly and the specificity of some of these reagents for β-Cys^{239}, our low-resolution mapping, and the intriguing similarities between the tubulin−colchicine complex and NTb preferential stabilization of minus ends suggest that β-Cys^{239} is the critical NEM-reactive residue. Alternatively, it remains possible that the critical NEM-reactive Cys is one of the as-yet-unidentified residues on α-tubulin, or even that minus end capping is due to modification of an α-Cys residue while plus end inhibition is due to modification of a β-Cys residue. However, if β-Cys^{239} is the critical NEM-reactive residue, then the proximity of this residue to the intradimer interface (*23*) suggests that NEM modification may either induce or prevent a conformational change that interferes with intradimer interactions. This disruption may in turn alter the longitudinal and/or lateral contacts between NTb and PCTb at the MT end.

In conclusion, individual MTs exposed to various NTb/PCTb mixtures were observed in real time, and the results indicate that NTb interacts with elongating plus and minus ends, and preferentially inhibits minus end assembly by a reversible capping mechanism. The ability of NTb to differentially affect tubulin association and dissociation at the two ends, and to uncouple catastrophe frequency from the rate of elongation specifically at the minus end, suggests that NTb may serve as a useful probe of differences in dynamic instability at the two ends. The experiments described in this paper focused on MT elongation and rapid shortening, and future work will involve analysis of NTb effects on MT transition frequencies, conclusive identification of the critical NEM-reactive residues on both α- and β-tubulin, and examination of NEM effects on tubulin conformation.

ACKNOWLEDGMENT

We thank Dr. Lynne Cassimeris, Bettina Deavours, and Arzu Karabay for critical review of the manuscript.

REFERENCES

1. Mitchison, T. (1993) *Science 261*, 1044−1047.
2. Fan, J., Griffiths, A. D., Lockhart, A., Cross, R. A., and Amos, L. A. (1996) *J. Mol. Biol. 259*, 325−330.
3. Mitchison, T., and Kirschner, M. (1984) *Nature 312*, 237−242.
4. Horio, T., and Hotani, H. (1986) *Nature 321*, 605−607.
5. Walker, R. A., O'Brien, E. T., Pryer, N. K., Soboeiro, M. F., Voter, W. A., Erickson, H. P., and Salmon, E. D. (1988) *J. Cell Biol. 107*, 1437−1448.
6. Desai, A., and Mitchison, T. J. (1997) *Annu. Rev. Cell Dev. Biol. 13*, 83−117.
7. Cassimeris, L. (1999) *Curr. Opin. Cell Biol. 11*, 134−141.
8. Kuriyama, R., and Sakai, H. (1974) *J. Biochem. 76*, 651−654.
9. Mann, K., Giesel, M., and Fasold, H. (1978) *FEBS Lett. 92*, 45−48.
10. Deinum, J., Wallin, M., and Lagercrantz, C. (1981) *Biochim. Biophys. Acta 671*, 1−8.
11. Huitorel, P., and Kirschner, M. W. (1988) *J. Cell Biol. 106*, 151−159.
12. Hyman, A., Drechsel, D., Kellogg, D., Salser, S., Sawin, K., Steffen, P., Wordeman, L., and Mitchison, T. (1991) *Methods Enzymol. 196*, 478−485.
13. Howard, J., and Hyman, A. A. (1993) *Methods Cell Biol. 39*, 105−113.
14. Luduena, R., and Roach, M. (1991) *Pharmacol. Ther. 49*, 133−152.
15. Kuriyama, R. (1976) *J. Biochem. 80*, 153−165.
16. Mellon, M. G., and Rebhun, L. I. (1976) *J. Cell Biol. 70*, 226−238.
17. Ikeda, Y., and Steiner, M. (1978) *Biochemistry 17*, 3454−3459.
18. Luduena, R. F., and Roach, M. C. (1981) *Biochemistry 20*, 4444−4450.
19. Basusarkar, P., Chandra, S., and Bhattacharyya, B. (1997) *Eur. J. Biochem. 244*, 378−383.
20. Wessel, D., and Flugge, U. I. (1984) *Anal. Biochem. 138*, 141−143.
21. Bai, R. L., Lin, C. M., Nguyen, N. Y., Liu, T. Y., and Hamel, E. (1989) *Biochemistry 28*, 5606−5612.
22. Walker, R. A., Pryer, N. K., and Salmon, E. D. (1991) *J. Cell Biol. 114*, 73−81.
23. Nogales, E., Wolf, S. G., and Downing, K. H. (1998) *Nature 391*, 199−203.

24. Bai, R., Choe, K., Ewell, J. B., Nguyen, N. Y., and Hamel, E. (1998) *J. Biol. Chem. 273*, 9894−9897.
25. Little, M., and Luduena, R. F. (1987) *Biochim. Biophys. Acta 912*, 28−33.
26. Shivanna, B. D., Mejillano, M. R., Williams, T. D., and Himes, R. H. (1993) *J. Biol. Chem. 268*, 127−132.
27. Bai, R., Ewell, J. B., Nguyen, N. Y., and Hamel, E. (1999) *J. Biol. Chem. 274*, 12710−12714.
28. Bai, R., Pei, X.-F., Boye, O., Getahun, Z., Grover, S., Bekisz, J., Nguyen, N. Y., Brossi, A., and Hamel, E. (1996) *J. Biol. Chem. 271*, 12639−12645.
29. Little, M., and Luduena, R. F. (1985) *EMBO J. 4*, 51−56.
30. Wolff, J., Knipling, L., Cahnmann, H. J., and Palumbo, G. (1991) *Proc. Natl. Acad. Sci. U.S.A. 88*, 2820−2824.
31. Uppuluri, S., Knipling, L., Sackett, D. L., and Wolff, J. (1993) *Proc. Natl. Acad. Sci. U.S.A. 90*, 11598−11602.
32. Shan, B., Medina, J. C., Santha, E., Frankmoelle, W. P., Chou, T. C., Learned, R. M., Narbut, M. R., Stott, D., Wu, P., Jaen, J. C., Rosen, T., Timmermans, P. B., and Beckmann, H. (1999) *Proc. Natl. Acad. Sci. U.S.A. 96*, 5686−5691.
33. Margolis, R. L., and Wilson, L. (1977) *Proc. Natl. Acad. Sci. U.S.A. 74*, 3466−3470.
34. Bergen, L. G., and Borisy, G. G. (1983) *J. Biol. Chem. 258*, 4190−4194.
35. Panda, D., Daijo, J. E., Jordan, M. A., and Wilson, L. (1995) *Biochemistry 34*, 9921−9929.
36. Bergen, L. G., and Borisy, G. G. (1986) *J. Cell. Biochem. 30*, 11−18.
37. Lin, C. M., Ho, H. H., Pettit, G. R., and Hamel, E. (1989) *Biochemistry 28*, 6984−6991.
38. Floyd, L. J., Barnes, L. D., and Williams, R. F. (1989) *Biochemistry 28*, 8515−8525.
39. Ponstingl, H., Krauhs, E., Little, M., and Kempf, T. (1981) *Proc. Natl. Acad. Sci. U.S.A. 78*, 2757−2761.
40. Krauhs, E., Little, M., Kempf, T., Hofer-Warbinek, R., Ade, W., and Ponstingl, H. (1981) *Proc. Natl. Acad. Sci. U.S.A. 78*, 4156−4160.

BI992200X